photonics

MDPI

Review

GaN-Based VCSELs with A Monolithic Curved Mirror: Challenges and Prospects

Tatsushi Hamaguchi

Compound Semiconductor Development Department, Research Division 3, Sony Semiconductor Solutions Corporation, 4-14-1 Asahi-cho, Atsugi-shi 243-0014, Kanagawa, Japan; tatsushi.hamaguchi@sony.com

Abstract: In this paper, we introduce how gallium nitride-based (GaN-based) VCSELs with curved mirrors have evolved. The discussion starts with reviewing the fundamentals of VCSELs and GaN-based materials and then introducing the curved-mirror cavity's principle and history and the latest research where the structure is applied to GaN-based materials to form VCSELs. We prepared these parts so that readers understand how VCSELs with this cavity work and provide excellent characteristics such as efficiency, life, stabilized mode behavior, etc. Finally, we discussed the challenges and prospects of these devices by touching on their potential applications.

Keywords: VCSEL; gallium nitride; blue; green; curved mirror

1. Introduction

Semiconductor lasers become operable when the light and carriers are confined to a small part of the semiconductor chip. Vertical cavity surface-emitting lasers (VCSELs [1]) are one of the most successful structures that enable semiconductor lasers, and a GaAs-based material system is almost ideal for fabricating VCSELs. The alternative lamination of AlGaAs layers having different Al content forms highly reflective mirrors and distributed Bragg reflectors (DBRs) [2] with electric conductivity. Forming quantum wells between two DBRs enables the efficient vertical resonance of light. The lateral oxidization of the AlAs layer formed close to quantum wells provides the horizontal confinement of light and carriers relative to the center of the device [3]. Combining these structures enables the efficient operation of GaAs-based VCSELs. By conducting intensive research on this kind of laser, the device can pave the way toward industrial success with applications such as sensors, printers, optically defined communication, and so on [4].

We have defined the emission wavelength of semiconductor devices by the band gaps of the active region used for photon generation. To attain the efficient vertical confinement of carriers to wells, the band gaps of barrier materials must be wide enough compared to the band gaps of wells. Moreover, to make VCSELs, the materials used for DBRs must also possess wider band gaps. These restrictions result in a gallium nitride (GaN) material system, with wider band gaps than conventional material systems such as AsP-based semiconductors, which is an adequate choice for making VCSELs with wavelengths shorter than red light (see Figure 1). The large offset between AlN, GaN, and InN's band gap enables efficient carrier confinement to their quantum wells. Pairing GaN and AlN, for example, enables the formation of DBRs that are transparent to these wavelengths [5].

However, the fabrication of GaN-based VCSELs is not necessarily easy. Nitride with high aluminum content suffers from high activation energy for p-type dopants [6], which toughens the formation of conductive p-type DBRs. Achieving conductivity with n-type GaN-based DBRs is still underway with respect to improvements in large band offsets between these materials [7]. These challenges compel researchers to use intracavity contacts covered by dielectric DBRs for the p-side [5,7] and to insert a relatively thick n-spacer between the quantum well and bottom-side DBRs to attain the current path from the n-side (see Figure 2a).

Citation: Hamaguchi, T. GaN-Based VCSELs with A Monolithic Curved Mirror: Challenges and Prospects. *Photonics* **2023**, *10*, 470. https://doi.org/10.3390/photonics10040470

Received: 14 February 2023
Revised: 12 April 2023
Accepted: 17 April 2023
Published: 20 April 2023

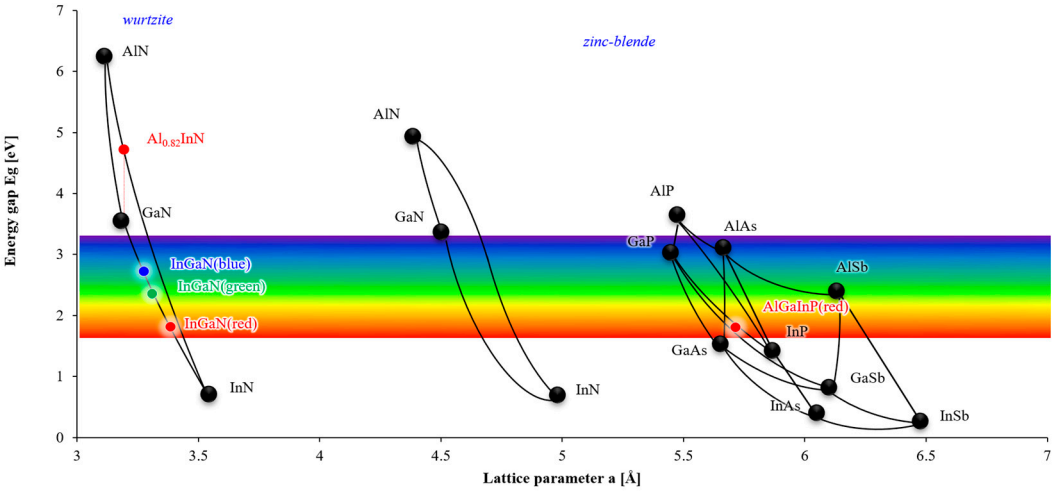

Figure 1. Band gap energy and lattice constant of compound semiconductors [8,9].

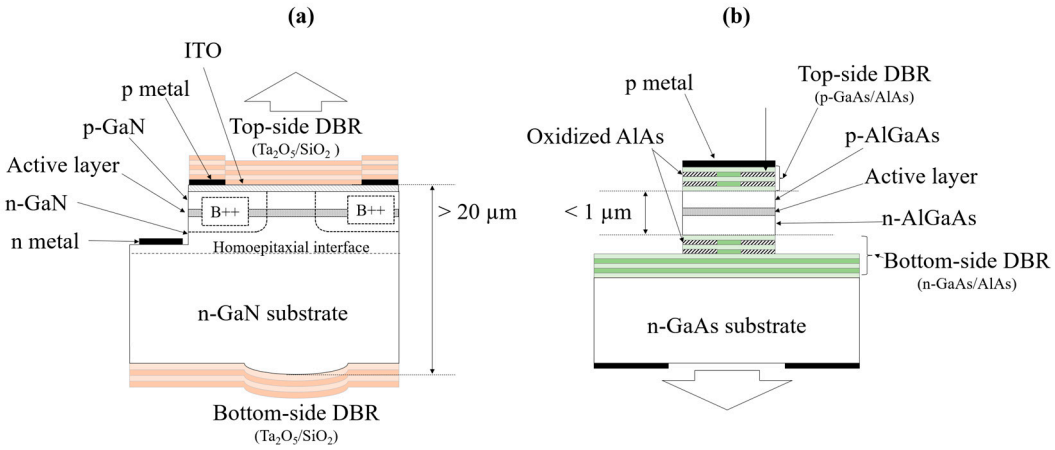

Figure 2. Schematic diagrams of (**a**) GaN-based VCSEL, the focus of this review, and (**b**) a typical GaAs-based VCSEL.

The lattice mismatch between materials introduces additional issues. The bulk GaN wafer, which we often use for laser fabrication, has a lattice mismatch relative to almost all semiconductor alloys of nitrides. Thus, these materials' lamination often leads to cracks in the epi wafer. $Al_{0.8}In_{0.2}N$ [10], without such a mismatch to GaN, is virtually the only choice, although it has other difficulties. This material presents spinodal decomposition, which causes the modulation of Al content [11] and roughens the layer's surface [12]. Although Al's high affinity to oxide facilitates lateral oxidation, the modulation of Al content causes inhomogeneous patterns after oxidation [13] that complicate adopting this approach when forming the apertures of VCSELs. Because the refractive index difference between GaN and AlInN is limited to a few percent, DBR obtained these materials by lamination, and they possess narrow stopbands of around 10–20 nm. Thus, making VCSELs with this DBR requires delicate control when the thickness of layers is less than 1% [14].

As discussed above, all component-enabled GaAs-based VCSELs, such as electrically conductive DBRs, and lateral confinement structures for light and carriers cannot be easily obtained with GaN-based VCSELs, driving some scientists to find improved approaches for VCSEL fabrication with GaN. For example, in situ monitoring for the precise thickness control of semiconductor DBRs could be a straightforward option. Despite these difficulties, the literature reported a high efficiency of 10% or more, with GaN-based VCSELs having dielectric DBRs at the top and semiconductor DBRs at the bottom [15,16]. This structure has two types of DBR materials in a single cavity called hybrid-DBR VCSELs.

The utilization of bottom-side semiconductor DBRs to broaden their stopband width is receiving popular research interest. The porous DBR is still showing relatively low peak reflectivity and a weak output power of less than a milliwatt [17,18], which indicates that this approach is on its way toward further sophistication.

Another approach is adopting all-dielectric DBRs, where both top and bottom side DBRs are made of dielectric materials, featuring a wider stopband associated with a larger refractive index difference between dielectric materials. These types of VCSELs originated from infrared VCSELs that are reported in the early stage of VCSEL history where both side mirrors comprised deposited metal layers [19], but this was gradually ignored. In the history of GaN-based VCSELs, this also became popular in the early stage of its research, which was conducted by companies and universities in 2008 [20]. However, most of these companies have not shown reports with this structure in this decade. The issue lies in its fabrication process. In the fabrication process, the deposition of top-side DBRs is followed by lapping the bottom side of the wafer and the formation of the bottom-side DBR, in which substrate thinning determines the cavity length. Considering diffraction loss, a cavity length that is as short as a few microns is preferable for suppressing the loss to less than 1% per round trip. However, thinning a wafer down to such thicknesses from initial values of around 300–400 µm is often associated with the introduction of cracks into the wafer.

The all-dielectric structure has merits in that it has a wide stopband, and it has drawbacks with respect to the stability of the fabrication process. On the other hand, such a short cavity has a mode spacing of around 10–20 nm, which is as wide as the gain spectrum of InGaN quantum wells. Thus, cavity length must be precisely controlled by the thinning process to locate the longitudinal modes in order to closely reach the peak of gain, further spoiling the fabrication process's robustness. This issue seemingly has been limiting the efficiency of such devices to less than 1%, which is considerably lower than the values reported with hybrid VCSELs.

Another issue with the structures mentioned above lies in heat management since the materials used for the DBRs of GaN-based VCSELs, semiconductors, and dielectric DBRs have low thermal conductivity around a few WmK^{-1} s. While GaN, filling the cavity, has a higher thermal conductivity of 130 WmK^{-1} s (please see Table 1), indicating that the heat exhaust is virtually only via GaN, a longer cavity provides better thermal conditions. A report revealed that the extension of the cavity ranged from a few microns to several halves of the thermal resistance of GaN-based VCSELs [21]. However, since we have limited the cavity length of all-dielectric and hybrid DBR VCSELs to a few microns to void the diffraction loss, all these structures have heat management issues.

Table 1. Example of thermal conductivity for materials used for GaN-based VCSELs.

Materials	Thermal Conductivity (W mK^{-1})
SiO_2	1.5
SiN	1.6
GaN	130
$Al_{0.84}InN$	4.5

2. Background of the Cavity with Curved Mirror

Among various challenges, this paper reviews the research of all-dielectric VCSELs with monolithic curved mirrors to solve the problems mentioned in the previous section.

Kogelnik et al. reported that a cavity with a flat and curved mirror at the end forms a stable laser resonator [22]. We can unfold this kind of cavity into an imaginary cavity with two curved mirrors and a twice-as-long cavity such as the original cavity, where the beam's waist is at the midpoint of the cavity. Thus, looking back at the original cavity with a flat and curved mirror, this cavity should form the beam waist on the flat mirror. There are two merits to the use of this cavity configuration. One is the implementation of lateral optical confinement, and the another implements stability against geometrical disturbances thanks to the oval shape of the mirror. Because the former suppresses the diffraction loss

of light traveling in the cavity, we can set a one-meter-long cavity without the dissipation of light. The latter eliminates the effect of a misaligned light path caused by geometrical disorders such as mirror tilting. Thus, researchers have commonly used this configuration in experiments on optical benches and set resonators with curved and flat mirrors that often extend to several meters or so, essentially with the positioning errors of components being derived from manual settings. These abilities of the curved–flat configuration provide efficient cavities even in such a situation. Additionally, this configuration is often used for external-cavity lasers to eliminate the diffraction loss caused by a relatively long cavity.

Iga et al. reported LED emissions from InP-based vertical cavities with a flat and a monolithic curved mirror as early as 1978 [23], which was investigated in one trial for VCSEL operations [24]. The application of this cavity to VCSELs has been rare (see Figure 3). In this study, Iga adopted a unique process to make the curved mirror: (i) patterning the resistance disk via photolithography on the substrate, (ii) turning the disks into droplets by heating, (iii) applying reactive ion etching using the resistance disk as a sacrificing mask that relieves the shaped drops onto the semiconductor substrate itself, and (iv) depositing dielectric DBRs onto the semiconductor substrate using vacuum deposition. This process, now popular for on-chip lens fabrication, is used for all formations of curved mirrors, which will be introduced later in this article.

In 2003, Park et al. reported the optically pumped laser operation of a GaN-based vertical laser with a monolithically curved mirror formed on the back side of a sapphire substrate used for GaN growth [25]. In 2004, Aldaz et al. reported the operation of a GaAs-based vertical laser with a curved mirror that is monolithically formed on the back side of the glass plate attached to a GaAs-based half-VCSEL [26]. In these two cases, they introduced intra-cavity interfaces between substrates and materials consisting of the active region that is associated with drastic refractive index gaps and the disturbance of vertical resonation. Even though these presented laser action, such interfaces seemingly caused high thresholds at 160 kW/cm^2 and 20 mA [16,17]. Such an interface also triggers controversial discussions about whether these should be considered VCSELs or VECSELs. Thus, one effective approach is to fill such cavities with substantially uniform materials.

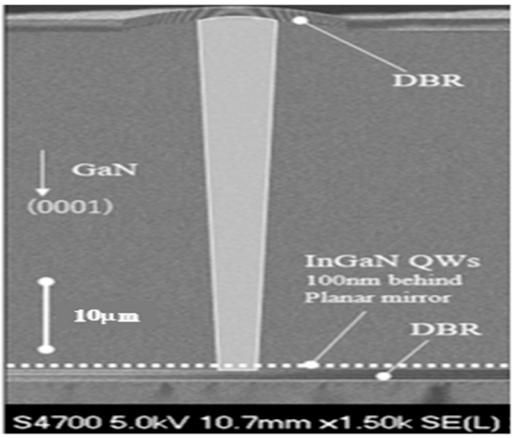

Figure 3. The cross-sectional SEM image of GaN-based VCSELs with curved mirrors [27].

3. Design of the Cavity with a Curved Mirror

The author relates the cavity's dimension to the resonant modes' lateral optical behavior. An analytical formulation describing the waist size of a Gaussian beam was given by Kogelnik [22]:

$$\sigma = \frac{1}{2}\sqrt{\frac{\lambda}{n\pi}\sqrt{LR - L^2}}$$

where σ is the standard deviation of the Gaussian profile, n is the equivalent refractive index of the cavity medium, L is the cavity length, and R is the radius of curvature of the curved mirror. This is the critical formula used to determine the lateral behavior of resonant modes in this type of cavity. R must be larger than L to form a stable resonator required by laser operations. When R is larger than L, this cavity provides a beam waist with stable resonance. Moreover, this cavity offers firm control for the beam waist size. Figure 4a,b calculate beam waist sizes via the formula above. Differentiating the abovementioned formula, "$R = 2L$" is obtained as a condition that makes $d\sigma/dL = 0$. Figure 4a illustrates that the beam waist is relatively indifferent to L when $R = 2L$. Figure 4b shows how it depends on R. For example, the figure roughly interprets that a 10% shift in R causes a change in the beam waist only in the order of 0.01 µm for many cases. Since the emission angle of the device is reciprocal to the size of the beam waist, such a minor error in σ will have a negligible impact on emission angles. Thus, once R is set larger than L, hopefully around $2L$, the near-field pattern (NFP) and far-field pattern (FFP) will be stable against dimensional disturbances.

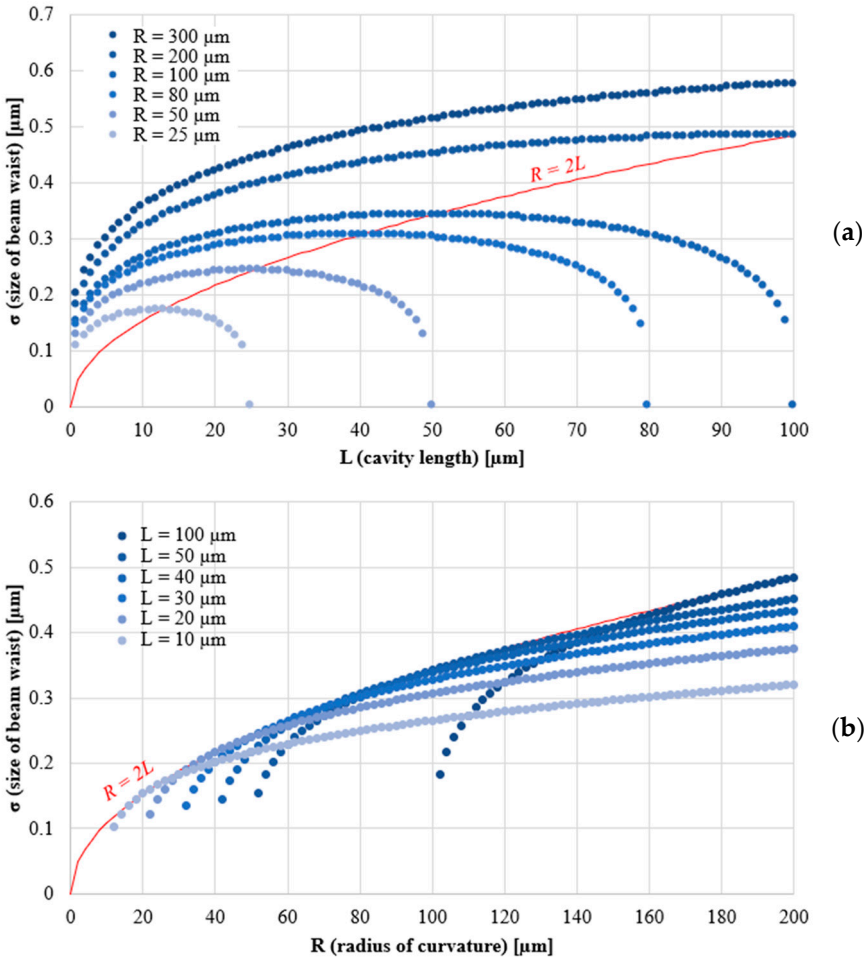

Figure 4. Simulated results show how the beam waist in a curved mirror cavity depends on (**a**) its cavity length and (**b**) the curved mirror's radius of curvature.

Another issue is the longitudinal behavior of resonant modes. The resonant wavelength meets

$$\lambda = \frac{nL}{2m}$$

where m is an arbitrary integer. Thus, we should control cavity length L so that λ is subsumed by the net gain spectrum of the device, whereas the extension of the cavity relaxes this restriction. The longitudinal mode spacing, $\Delta\lambda$, is obtained by the following.

$$L = \frac{\lambda^2}{2n\Delta\lambda}\left(1 - \frac{\lambda}{n}\frac{dn}{d\lambda}\right)^{-1}$$

Figure 5 shows an example of the relation between the longitudinal mode spacing and cavity length. In this case, for example, $L > 10$ μm, the longitudinal mode spacing reduces to less than a few nanometers and further reduces with the extension of the cavity length. In such conditions, the longitudinal mode spacing can be narrower than the width of the net gain spectrum of semiconductor quantum wells, enabling one mode to exploit the gain and automatically become dominant without the precise control of the cavity's length.

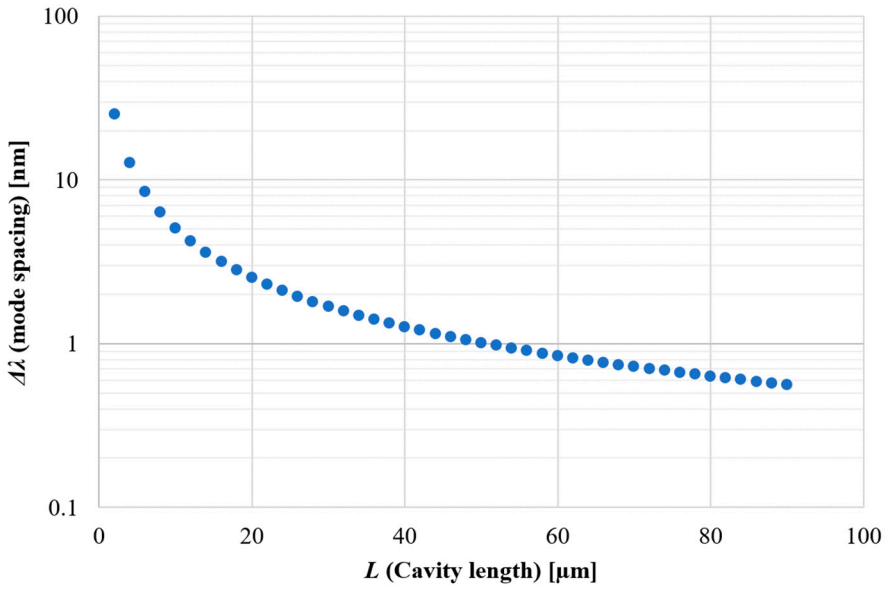

Figure 5. Simulated results to show how longitudinal mode spacing depends on the cavity length, where λ = 445 nm, $dn/d\lambda = -0.001$, and n = 2.45 were used.

To summarize the discussion in this section, VCSELs with curved mirrors with dimensions that meet the below information would possess a stable resonance required for lasing:

- $R > L$, hopefully around $2L$;
- $L > 10$ μm.

4. Blue and Green VCSELs

The author's group has been reporting that GaN-based VCSELs' operations meet the conditions. Aside from the first report of operation under pulsed current injections in 2018 [27], reports on blue VCSELs with this structure exist: efficient current confinement by ion-implantation [28], sub-mill ampere operation [29], stabilized lateral modes [30], and high-efficiency operation up to 13.5% [31] (see Figure 6a); long duration of life reaching 2000 h [32]; and narrow emission angle of 3.9 degrees for circular apertures [33] and 0.5 degrees for oblong apertures [34]. Recently, the present group has also reported the CW operation of green VCSELs [35], milliwatt class outputs, and its high-efficiency operation [36] (see Figure 6b). The present group also demonstrated white illumination by combining lasers from blue, green, and red VCSELs [35]. Additionally, we observed spatially coherent dot generation associated with a sub-degree emission angle for a similar structure [34].

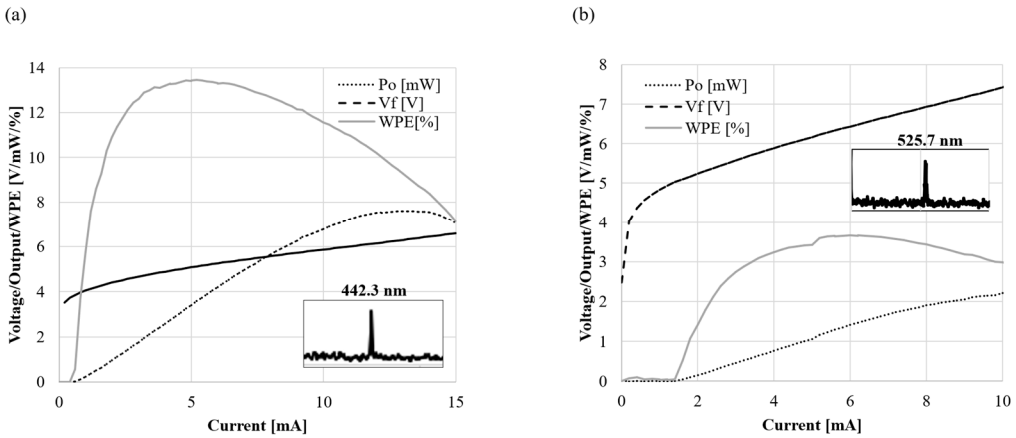

Figure 6. I-V/L and I-WPE curves of (**a**) blue [31] and (**b**) green VCSELs [36] with a curved mirror. The insets are the emission spectra obtained from the above threshold currents.

The series of research revealed the merits of this cavity structure. As evidence of the fabrication stability against dimensional errors, a 100% yield of lasing and the high uniformity of I-V/L have been reported. The standard deviation of I_{th} and the maximum output power was 6.1% and 5.1%, respectively [31]. Figure 7 shows the updated data on the uniformity of blue VCSELs with a curved mirror. It shows that 55 chips showed uniform I-V and I-L, and the calculated maximum efficiency among these was about 15%. We obtained these chips in a centimeter-wide area. Figure 8 shows how the I_{th} of GaN-based VCSELs is dependent on the wavelength. VCSELs with curved mirrors show a low threshold current, which is another piece of evidence for this cavity's superiority, such as its ability to eliminate diffraction loss.

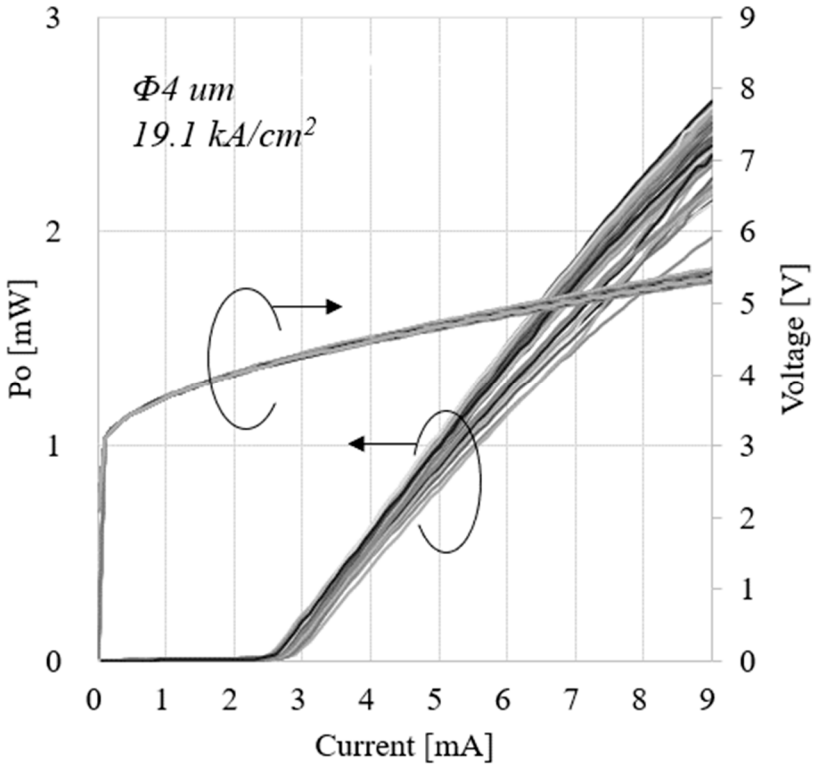

Figure 7. The I-V and I-L characteristics of curved mirror blue VCSELs. It contains data for 55 chips obtained from a wafer.

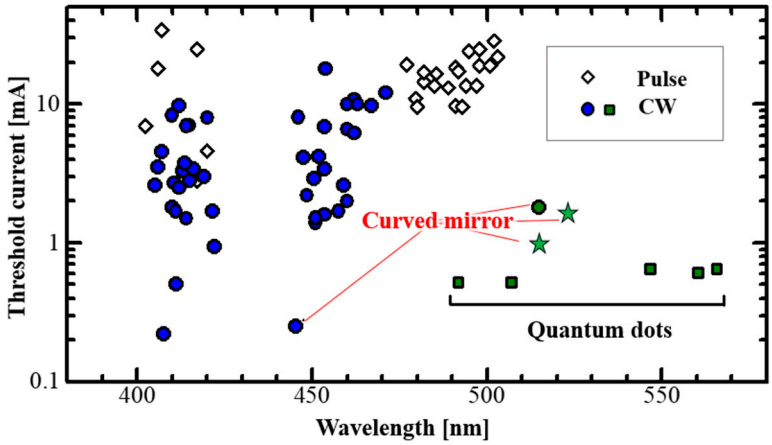

Figure 8. Plot to show how the threshold current of GaN-based VCSELs depends on the wavelength. This is based on Hatakoshi' s plot [4,37] and redrawn by the present author adding new plots that appears as stars.

5. Applications

We achieved full-color displays for LEDs and edge-emitting lasers by combining GaN-based blue- and green-light-emitting devices with GaAs-based red-light-emitting devices. The same results, therefore, can be expected for VCSEL. In particular, low power consumption, which is the greatest benefit of VCSELs, contributes to the reduction in battery capacity, leading to a decrease in the form factors of these devices. A full-color retinal scanning display is an example in which VCSELs seem suitable for applications [38], a type of AR/VR mobile terminal in which an image is obtained by directly scanning the retina with a laser beam. We expect to use this application for entertainment and medical purposes, such as improving the eyesight of patients affected by amblyopia. We can obtain sufficiently bright images by projecting a laser at approximately μW-class level to the eye. However, we must conduct safety measures to avoid damage to the retina. VCSELs with a small output can simultaneously achieve sufficient luminance and safety. This kind of display, which does not use VCSEL, is already on the market [39] and is often mentioned in academic societies as a future application of GaN VCSEL.

Meanwhile, laser projectors have promising applications. In devices using edge-emitting lasers, which are currently widely distributed in the market, the emitted laser is subjected to fine irregularities on the screen surface, resulting in interference and producing luminance unevenness, called speckle noise, which degrades the image quality of displays. The interference becomes blunt by arraying a plurality of VCSEL elements with slightly different wavelengths, reducing the speckle noise [40]. Furthermore, we may increase the number of arrays to enhance the output, leading to a larger and brighter projection image. Additionally, Since the VCSEL array can be used as a display as it is, using VCSEL arrays might not require any external components such as LCD panels or MEM mirrors to provide images and will further compact the laser projector.

Apart from displays, there are a variety of potential applications for GaN-based VCSELs mentioned in papers: optical communication via plastic optical fiber, biosensors, 3D printers, atomic clocks, illumination, laser cutters, and so on [41]. All these use VCSEL's ability, which allows low power consumption, high-frequency operation, and arraying.

6. Challenge and Prospects

6.1. Longitudinal Mode Control

Although applications are waiting for the advent of visible VCSELs in the industry, challenges remain. One issue is a lack of longitudinal mode control. The extremely long cavity of the device often leads to multimodal emission or mode hopping during operations, which is a drawback for certain applications, as atomic clocks or any devices with components require severe wavelength sensitivity. In 2022, we allowed an etalon

with considerable modulation in the reflectivity spectrum to replace one of the DBRs and observed the firm stabilization of emission wavelengths with a side mode suppression ratio (SMSR) of 40 dB or more [32]. The reflectivity modulation of the etalon imposes different degrees of optical penalty to each longitudinal mode and automatically selects one with the lowest penalty (see Figures 9 and 10). By setting the peak reflectivity to as high as 99%, we can attain the stabilization of longitudinal modes with mill-watt class output power. The research on this topic is in its preliminary phase and leaves a minor issue. For example, the etalon itself exhibits a minor absorption of light, which sometimes, for example, halves the slope efficiency [42].

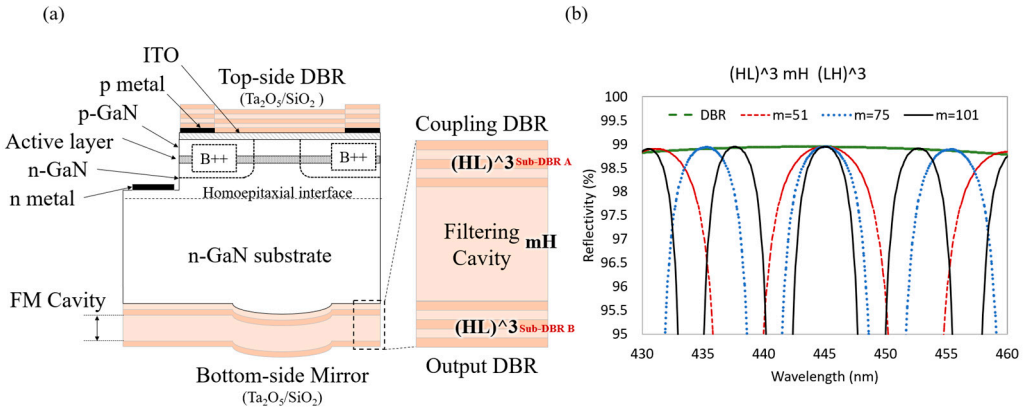

Figure 9. The schematic of a curved mirror VCSEL (**a**) with a bottom-side filtering mirror. The reflectivity spectrum of three different filtering mirrors (**b**) with a reference wavelength of 445 nm and cavities of m = 51, 75, and 101.

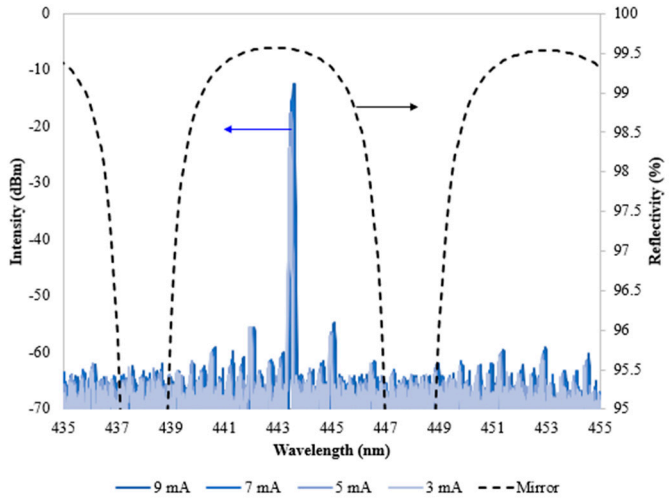

Figure 10. The emission spectrum of curved mirror VCSELs with a filtering mirror. The longitudinal modes are stable across multiple operating conditions regardless of the nanometer narrow mode spacing due to a long cavity that is >20 μm.

6.2. Polarization Control

Another issue is the lack of polarization control since gallium nitride has a hexagonal crystal and the substrate used for device fabrication usually has a surface parallel to the basal plane, which is {0001} of GaN. The basal plane has a high degree of hexagonal symmetry, so the device fabricated over there has no certain preference for polarization and tends to have an arbitrary direction. We reported that the usage of the semi-polar {20–21}, a plane of GaN that has lower symmetry (see Figure 11), is effective in locking the polarization direction of the device [26]. Currently, the {0001} substrate is the most popular for industrial use, while {20–21} is less popular. Thus, finding a practical approach

to polarization control with {0001} is essential to quickly put the device into practical use. There could be possible approaches for its application, such as applying mechanical stress to quantum wells.

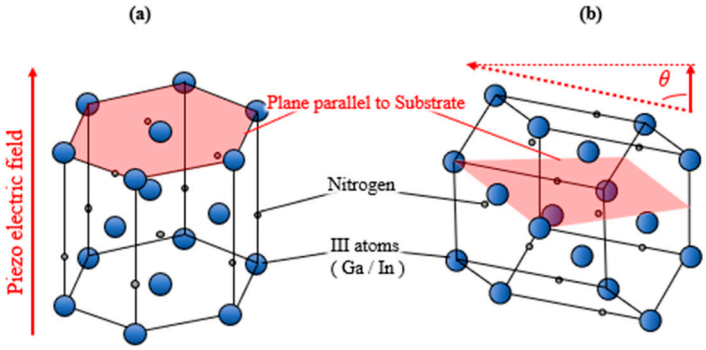

Figure 11. (**a**) The {0001}-orientated, or so-called c-orientated, lattice is shown. (**b**) The {20–21}-orientated lattice is shown. The {20–21} lattice is obtained by rotating the {0001} lattice by 75 degrees towards the m direction. The rotation of the crystal reduces the piezoelectric field normal to the substrate, thereby suppressing the QW degradation for high indium incorporation.

6.3. Efficiency

The efficiency of GaN-based VCSELs is relatively low among the types of light emitters. The scientific and quantitative discussion of the marginal performance of the device is still underway. This section tries to observe the perspective of the efficiency of GaN-based VCSELs via an empirical approach. Figure 12 shows the trend of the wall plug efficiency of blue LEDs, edge-emitting lasers (EELs), and VCSELs. This figure illustrates that the improvement in VCSELs is at a similar pace as the past pace of EELs. That may give one the impression that VCSEL's efficiency will follow this trend in the coming years, hopefully at around 40% in 2030.

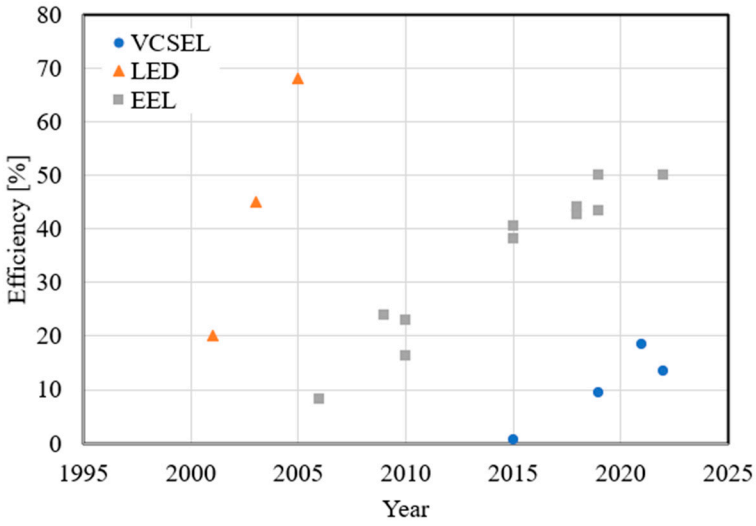

Figure 12. Efficiency trend of blue LED, EEL, and VCSELs (courtesy of T. Miyamoto and M. Kuramoto).

Reading how the efficiencies of EELs and VCSELs depend on wavelengths leads us to another point (see Figure 13). This trend illustrates two aspects; (i) the efficiency of VCSELs is lower than EELs for all ranges of wavelengths, and (ii) the degree of behind in efficiency is relatively considerable for shorter and longer wavelengths. Discussion around the cause of this generally requires complicated analyses considering various parameters. One aspect of simplifying the discussion is remarking on the geometrical difference in these devices' electrical (carriers) and optical (photons) paths. They are parallel and have more geometric

overlap in VCSELs. At the same time, they are orthogonal, and have less overlap in EELs, enhancing the optical impact in VCSELs associated with implementing current paths. For instance, one significant way to establish conductivity is doping on semiconductors. This is associated with plasma absorption, which is generally prominent in the infrared region and diminishes in the near-infrared region. This is consistent with the trend that VCSELs have greater plasma absorption relative to EEL around the region between 1.2 and 1.6 mm. Looking back at GaN-based VCSELs, although plasma absorption is negligible, the inter-band absorption of materials is serious. Intracavity contacts are required to circumvent electrically insulated DBRs. For instance, indium tin oxide (ITO) is often the current path at the top side. ITO's inter-band transition causes a certain amount of loss even at visible regions, which degrades the cavities' Q factor to reduce efficiency [43]. Recent research is reporting structures where the tunnel junction (TJ) and n-GaN current spreader replaces ITO, and such a structure reduces optical loss toward better I-L curves [44]. One issue with introducing TJ has been an operational voltage increase that is as considerable as around or over one volt, which is caused by the wide band gaps of nitride materials. Recently, the voltage was reduced to as low as standard VCSELs with ITO [45]. Additionally, a report indicated that VCSELs with TJ have a longer life than those with ITO [46].

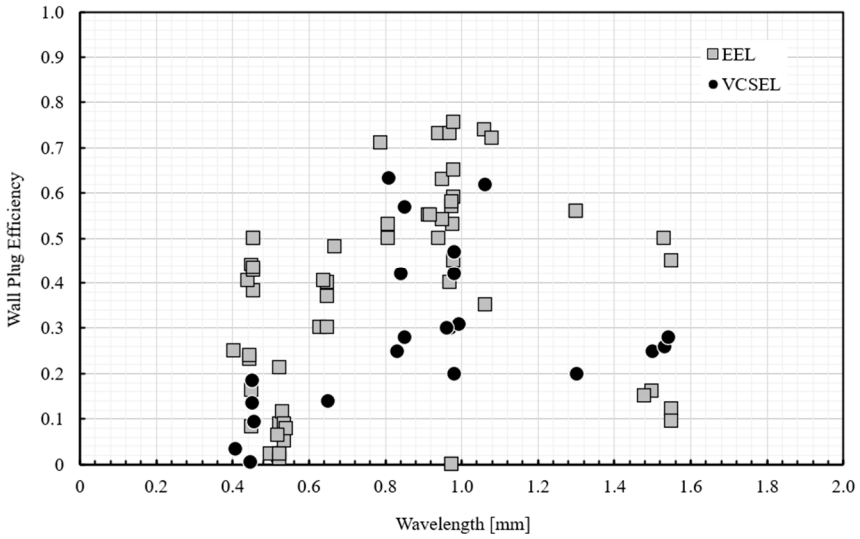

Figure 13. Efficiency dependence on wavelength (courtesy of T. Miyamoto).

6.4. Lineup of Colors

Taking that one potent application for visible VCSELs as a display, we must consider how all three colors, blue, green, and red, can be attained in order to introduce them into the market. In GaN-based laser research, the study related to blue colors has been the most intensive and shows the best characteristics such as power (>10 mW), efficiency (>10%), and life (>2000 h) [32]. At the same time, green shows a power of only around 3 mW, an efficiency around of 3% [47], and no report on its life. We predicted that green VCSELs should be prepared for practical use later than blue VCSELs. The cause of the delay in research of GaN-based green VCSELs is a (i) large lattice mismatch between InGaN multiquantum wells (MQWs) for green emission and GaN used for device fabrication, which causes defects to deteriorate emission efficiency; (ii) mechanical stress in MQW, which enhances the piezoelectric field to separate the hall and electron and degrades emission efficacy [48]; and the (iii) relatively high vapor pressure of InN that impedes the deposition of InGaN MQWs itself. All these become more serious when researchers try to add more In into InGaN MQWs for green emissions. This difficulty reduces the efficiency, power, and life of green-light-emitting devices and not only VCSELs, which is well known as the "green gap" in the solid-state lighting industry. As with EELs and LEDs, green emitters were less efficient than blue and red. Ultimately, however, efforts by

researchers have led to improvements in efficiency, leading to practical use. For VCSELs, for example, quantum dots [49] and semi-polar substrates [35] are currently used to realize green light emission, and we expect further progress with respect to overcoming the green light emission research gap completely.

Red VCSELs based on arsenide and phosphide materials have been reported in the 2000s. Since the GaN-based red light emitter is still on its way toward lasing [50–52], these materials are currently the most potent choice for VCSEL fabrication. The most serious issue is the small band offset in this material system, which becomes more remarkable for shorter emission wavelengths. Although this type of VCSEL shows a 12 mW output at 670 nm, it diminishes to 4 mW at 650 nm and diminishes below that value for shorter wavelengths [53]. Moreover, the small offset in a bad lineup leads to the devices' poor thermal stability, which prevents the device from entering the market. The industry must either wait for improvements in these arsenic-based devices or lasers based on new materials. GaN-based materials can have relatively high band barriers so that the temperature characteristics can be good. Recently, improvements in red GaN-based LEDs [50] have been reported, and long-wavelength directive emissions using nanowires have been obtained, but their wavelengths are still shorter than red light [51]. As another approach, Eu-doped GaN showed incredibly pure red emissions under the current injection [52]. Alternatively, we have observed an organic laser caused by current injection oscillations in recent years, and it may also be a candidate for a future red VCSEL [54].

6.5. Comparison between Structures

Table 2 shows a concise comparison between major structures reported for GaN-based VCSELs. One structure labeled "all-dielectric flat-mirror" showed relatively low efficiency and a considerably shorter lifetime. As stated in the Introduction, one issue behind this is the difficulties during the fabrication process. Two of them, the structures labeled "all-dielectric curved-mirror" and "hybrid flat-mirror," show relatively high efficiencies and lifetimes at >15% and >1000 h, respectively. This suggests that these are candidates that currently compete toward practical applications.

Table 2. Comparison between major structures reported for GaN-based VCSELs.

	All-Dielectric (Curved-Mirror)	**All-Dielectric (Flat-Mirrors)**	**Hybrid (Flat-Mirrors)**
Affiliation	Sony [27–36]	Nichia [20], UCSB [43,44], Xiamen [21,49], etc.	Meijo and Stanley [15], Nichia [16], NYCU [5], etc.
Bottom DBR	Dielectric (curved)	Dielectric (flat)	Semiconductor (flat)
Top DBR	Dielectric (flat)	Dielectric (flat/mesa)	Dielectric (flat/mesa)
Cavity length	10~50 um	A few microns	A few microns
Wall plug efficiency	>15%	~1%	>15%
Output power	>10 mW	~mW	>10 mW
Life	>1000 h	~minutes	>1000 h
Lasing yield	100%	Not reported	>80%
Colors	blue (c-plane) and green (semi-polar)	Blue (c-plane) Green (c-plane, quantum dot)	Blue (c-plane) Green (c-plane)

The apparent difference between them is the cavity length. The curved one is much longer than others, resulting in heat management advantages, as stated in the Introduction, which would be advantageous for making arrayed VCSELs for high power outputs where heat management is more important than in a chip with a single emitter.

Another apparent difference is the variety of substrate types. While hybrid types have been reported only over c-plane GaN, the curved mirror's VCSELs have been reported with multiple substrates, including semi-polar GaN. The curved mirror structure is material agnostic because we defined the curved structure by the shape of resin droplets formed

over the substrate. The droplets automatically form spherical surfaces during the reflowing process to reduce the surface's free energy; this mechanism is independent of the choice of the substrate. While, in the hybrid structure, the bottom DBR mirror consists of the lamination of interfaces between semiconductor layers that are directly formed on the substrate by epitaxial growth, the surficial morphology of the substrate naturally depends on the choice of materials. As discussed in Section 1, the material's characteristics traditionally play a key role in enabling VCSEL fabrication. This keeps the material systems used for VCSEL fabrication virtually only to AsP-based systems, with all components, conductive DBRs, lateral oxidation, etc., available. On the other hand, the curved mirror structure has unleashed this limitation, as we learned via the realization of VCSEL with gallium nitride, and this makes other researchers consider other curved mirror VCSELs with new materials. For example, we could even use organic materials with this approach [54].

7. Conclusions

In this paper, we described the evolution of curved mirror gallium-nitride-based (GaN-based) VCSELs. The discussion began with a review of the very principles of VCSELs and GaN-based materials, followed by an introduction to the theory, the background of the curved-mirror cavity, and the most recent research using this structure to create VCSELs. These sections explained how VCSELs with this cavity function offer great qualities such as efficiency, life, stabilized mode behavior, etc. Finally, by briefly mentioning some of these devices' prospective applications, the difficulties and prospects of these devices are examined.

Funding: This research was conducted as a part of Sony's research activity and received no external funding.

Acknowledgments: The author appreciates all efforts provided by the past and current colleagues: Maiko Ito, Jared A. Kearns, Tomohiro Makino, Kentaro Hayashi, Maho Ohara, Noriko Kobayashi, Tatsuro Jyokawa, Eiji Nakayama, Shouetsu Nagane, Koichi Sato, Yuki Nakamura, Yukio Hoshina, Masamichi Ito, Masayuki Tanaka, Hiroshi Nakajima, Jugo Mitomo, Susumu Sato, Hideki Watanabe, Hironobu Narui, Yuya Kanitani, Seiji Kasahara, Sumu Kusanagi, Yoshihiro Kudo, Rintaro Koda, Noriyuki Futagawa, Koya Otomo, and Yumina Mmisu. The author also greatly appreciates the insightful advice behind this paper given by Ken-ichi Iga, Fumio Koyama, Tomoyuki Miyamoto, Masaru Kuramoto, Tetsuya Takeuchi, Motoaki Iwaya, Katsumi Kishino, Atsushi A. Yamaguchi, Yasufumi Fujiwara, Chihaya Adachi, Kazuhiro Ohkawa, Steven Denbaas, and Shuji Nakamura.

Conflicts of Interest: The author declare no conflict of interest.

References

1. Iga, K. Vertical-Cavity Surface-Emitting Laser: Its Conception and Evolution. *Jpn. J. Appl. Phys.* **2008**, *47*, 1. [CrossRef]
2. Koyama, F.; Kinoshita, S.; Iga, K. Room Temperature CW Operation of GaAs Vertical Cavity Surface Emitting Laser. *Trans. IEICE Electron.* **1988**, *71*, 1089–1090.
3. Choquette, K.D.; Schneider, R.P., Jr.; Lear, K.L.; Geib, K.M. Low threshold voltage vertical-cavity lasers fabricated by selective oxidation. *Electron. Lett.* **1994**, *30*, 2043. [CrossRef]
4. Padullaparthi, B.D.; Tatum, J.; Iga, K. *VCSEL Industry: Communication and Sensing*; Wiley-IEEE Press: Hoboken, NJ, USA, 2021.
5. Lu, T.-C.; Kao, C.-C.; Kuo, H.-C.; Huang, G.-S.; Wang, S.-C. CW lasing of current injection blue GaN-based vertical cavity surface emitting laser. *Appl. Phys. Lett.* **2008**, *92*, 141102. [CrossRef]
6. Nam, K.B.; Nakarmi, M.L.; Li, J.; Lin, J.Y.; Jiang, H.X. Mg acceptor level in AlN probed by deep ultraviolet photoluminescence. *Appl. Phys. Lett.* **2003**, *83*, 878. [CrossRef]
7. Shibata, K.; Nagasawa, T.; Kobayashi, K.; Watanabe, R.; Tanaka, T.; Takeuchi, T.; Kamiyama, S.; Iwaya, M.; Kamei, T. High-quality n-type conductive Si-doped AlInN/GaN DBRs with hydrogen cleaning. *Appl. Phys. Express* **2022**, *15*, 112007. [CrossRef]
8. Vurgaftman, I.; Meyer, J.R.; Ram-Mohan, L.R. Band parameters for III–V compound semiconductors and their alloys. *J. Appl. Phys.* **2001**, *89*, 5815. [CrossRef]
9. Veal, T.D.; McConville, C.F.; Schaff, W.J. (Eds.) *Indium Nitride and Related Alloys*; CRC Press: Boca Raton, FL, USA, 2009.
10. Cosendey, G.; Carlin, J.-F.; Kaufmann, N.A.K.; Butté, R.; Grandjean, N. Blue monolithic AlInN-based vertical cavity surface emitting laser diode on free-standing GaN substrate. *Appl. Phys. Lett.* **2011**, *98*, 181111. [CrossRef]
11. Palisaitis, J.; Hsiao, C.-L.; Hultman, L.; Birch, J.; Persson, P.O. Direct observation of spinodal decomposition phenomena in InAlN alloys during in-situ STEM heating. *Sci. Rep.* **2017**, *7*, 44390. [CrossRef]

12. Butté, R.; Carlin, J.-F.; Feltin, E.; Gonschorek, M.; Nicolay, S.; Christmann, G.; Simeonov, D.; Castiglia, A.; Dorsaz, J.; Buehlmann, H.J.; et al. Current status of AlInN layers lattice matched to GaN for photonics and electronics. *J. Phys. D Appl. Phys.* **2007**, *40*, 6328. [CrossRef]
13. Dorsaz, J.; Bühlmann, H.-J.; Carlin, J.-F.; Grandjean, N.; Ilegems, M. Selective oxidation of AlInN layers for current confinement in III–nitride devices. *Appl. Phys. Lett.* **2005**, *87*, 072102. [CrossRef]
14. Hamaguchi, T.; Fuutagawa, N.; Izumi, S.; Murayama, M.; Narui, H. Milliwatt-class GaN-based blue vertical-cavity surface-emitting lasers fabricated by epitaxial lateral overgrowth. *Phys. Status Solidi* **2016**, *213*, 1170–1176. [CrossRef]
15. Kuramoto, M. High-Power GaN-Based Vertical-Cavity Surface-Emitting Lasers with AlInN/GaN Distributed Bragg Reflectors. *Appl. Sci.* **2019**, *9*, 416. [CrossRef]
16. Terao, K. Blue and green GaN-based vertical-cavity surface-emitting lasers with AlInN/GaN DBR. In *Gallium Nitride Materials and Devices XVI*; SPIE: San Francisco, CA, USA, 2021; p. 116860E.
17. Lee, S.-M. Optically pumped GaN vertical cavity surface emitting laser with high index-contrast nanoporous distributed Bragg reflector. *Opt. Express* **2015**, *23*, 11023–11030. [CrossRef] [PubMed]
18. Elafandy, R.T. Study and Application of Birefringent Nanoporous GaN in the Polarization Control of Blue Vertical-Cavity Surface-Emitting Lasers. *ACS Photonics* **2021**, *8*, 1041–1047. [CrossRef]
19. Soda, H.; Iga, K.-I.; Kitahara, C.; Suematsu, Y. GaInAsP/InP Surface Emitting Injection Lasers. *Jpn. J. Appl. Phys.* **1979**, *18*, 2329. [CrossRef]
20. Higuchi, Y.; Omae, K.; Matsumura, H.; Mukai, T. Room-Temperature CW Lasing of a GaN-Based Vertical-Cavity Surface-Emitting Laser by Current Injection. *Appl. Phys. Express* **2008**, *1*, 121102. [CrossRef]
21. Mei, Y. A comparative study of thermal characteristics of GaN-based VCSELs with three different typical structures. *Semicond. Sci. Technol.* **2018**, *33*, 015016. [CrossRef]
22. Kogelnik, H.; Li, T. Laser Beams and Resonators. *Appl. Opt.* **1966**, *5*, 1550. [CrossRef]
23. Iga, K.; Kambayashi, T.; Kitahra, C.; Wakao, K.; Moriki, K. GaInNAsP/InP double heterostructure planner LED's. *IEEE Trans. Electron. Devices* **1978**, *26*, 1227–1230. [CrossRef]
24. Iga, K.; Tokyo Institute of Technology, Yokohama, Japan. Personal communication. November 2022.
25. Park, S.-H.; Kim, J.; Jeon, H.; Sakong, T.; Lee, S.-N.; Chae, S.; Park, Y.; Jeong, C.-H.; Yeom, G.-Y.; Cho, Y.-H. Room-temperature GaN vertical-cavity surface-emitting laser operation in an extended cavity scheme. *Appl. Phys. Lett.* **2003**, *83*, 2121. [CrossRef]
26. Aldaz, R.I.; Wiemer, M.W.; Miller, D.A.B.; Harris, J.S. Monolithically-integrated long vertical cavity surface emitting laser incorporating a concave micromirror on a glass substrate. *Opt. Express* **2004**, *12*, 3967. [CrossRef] [PubMed]
27. Hamaguchi, T.; Tanaka, M.; Mitomo, J.; Nakajima, H.; Ito, M.; Ohara, M.; Kobayashi, N.; Fujii, K.; Watanabe, H.; Satou, S.; et al. Lateral optical confinement of GaN-based VCSEL using an atomically smooth monolithic curved mirror. *Sci. Rep.* **2018**, *8*, 10350. [CrossRef]
28. Hamaguchi, T.; Nakajima, H.; Ito, M.; Mitomo, J.; Satou, S.; Fuutagawa, N.; Narui, H. Lateral carrier confinement of GaN-based vertical-cavity surface-emitting diodes using boron ion implantation. *Jpn. J. Appl. Phys.* **2016**, *55*, 122101. [CrossRef]
29. Hamaguchi, T.; Nakajima, H.; Tanaka, M.; Ito, M.; Ohara, M.; Jyoukawa, T.; Kobayashi, N.; Matou, T.; Hayashi, K.; Watanabe, H.; et al. Sub-milliampere-threshold continuous wave operation of GaN-based vertical-cavity surface-emitting laser with lateral optical confinement by curved mirror. *Appl. Phys. Express* **2019**, *12*, 044004. [CrossRef]
30. Nakajima, H.; Hamaguchi, T.; Tanaka, M.; Ito, M.; Jyokawa, T.; Matou, T.; Hayashi, K.; Ohara, M.; Kobayashi, N.; Watanabe, H.; et al. Single transverse mode operation of GaN-based vertical-cavity surface-emitting laser with monolithically incorporated curved mirror. *Appl. Phys. Express* **2019**, *12*, 084003. [CrossRef]
31. Ito, M.; Hamaguchi, T.; Makino, T.; Hayashi, K.; Kearns, J.; Ohara, M.; Kobayashi, N.; Nagane, S.; Sato, K.; Nakamura, Y.; et al. Highly efficient operation and uniform characteristics of curved mirror Vertical-cavity surface-emitting lasers. *Appl. Phys. Exp.* **2022**, *16*, 012006. [CrossRef]
32. Kearns, J.A.; Hamaguchi, T.; Hayashi, K.; Ohara, M.; Makino, T.; Ito, M.; Kobayashi, N.; Jyoukawa, T.; Nakayama, E.; Nagane, S.; et al. Mode control in long cavity VCSELs with a curved mirror. In *Gallium Nitride Materials and Devices XVII*; SPIE OPTO: San Francisco, CA, USA, 2022; Volume 12001, p. 1200108.
33. Hayashi, K.; Hamaguchi, T.; Kearns, J.; Kobayashi, N.; Ohara, M.; Makino, T.; Nagane, S.; Sato, K.; Nakamura, Y.; Hoshina, Y.; et al. Narrow Emission of Blue GaN-Based Vertical-Cavity Surface-Emitting Lasers with a Curved Mirror. *IEEE Photonics J.* **2022**, *14*, 1536905. [CrossRef]
34. Hamaguchi, T.; Makino, T.; Hayashi, K.; Kearns, J.A.; Ohara, M.; Ito, M.; Kobayashi, N.; Nagane, S.; Sato, K.; Nakamura, Y.; et al. Spontaneously implemented spatial coherence in vertical-cavity surface-emitting laser dot array. *Sci. Rep.* **2022**, *12*, 21629. [CrossRef]
35. Hamaguchi, T.; Hoshina, Y.; Hayashi, K.; Tanaka, M.; Ito, M.; Ohara, M.; Jyoukawa, T.; Kobayashi, N.; Watanabe, H.; Yokozeki, M.; et al. Room-temperature continuous-wave operation of green vertical-cavity surface-emitting lasers with a curved mirror fabricated on {20−21} semi-polar GaN. *Appl. Phys. Express* **2020**, *13*, 041002. [CrossRef]
36. Ito, M.; Hamaguchi, T.; Makino, T.; Hayashi, K.; Kearns, J.A.; Ohara, M.; Kobayashi, N.; Nagane, S.; Sato, K.; Nakamura, Y.; et al. Latest progress of high-efficient blue and green VCSELs with curved mirror. PRJ3-1. In Proceedings of the 29th International Display Workshops, Fukuoka, Japan, 14 December 2022.
37. Hatakoshi, G.; Iga, K. *Principal and Application System of VCSELs (Written in Japanese)*, 2nd ed.; Design Egg Inc.: Tokyo, Japan, 2022.

38. Hamaguchi, T.; Hoshina, Y.; Jyokawa, T.; Ohara, M.; Hayashi, K.; Kobayashi, N.; Nagane, S.; Sato, K.; Nakamura, Y.; Kearns, J.; et al. 49-2: Invited Paper: Blue and Green VCSEL for Full-Color Display. In *Digest of Technical Papers—SID International Symposium*; 2021 held as an online event; Wiley: Hoboken, NJ, USA, 2021; Volume 52, pp. 677–679.
39. Available online: https://www.retissa.biz/ (accessed on 2 February 2023).
40. Kuroda, K.; Ishikawa, T.; Ayama, M.; Kubota, S. Color Speckle. *Opt. Rev.* **2014**, *21*, 83. [CrossRef]
41. Hamaguchi, T.; Tanaka, M.; Nakajima, H. A review on the latest progress of visible GaN-based VCSELs with lateral confinement by curved dielectric DBR reflector and boron ion implantation. *Jpn. J. Appl. Phys.* **2019**, *58*, SC0806. [CrossRef]
42. Kearns, J.A.; Hamaguchi, T.; Hayashi, K.; Ohara, M.; Makino, T.; Ito, M.; Kobayashi, N.; Jyoukawa, T.; Nakayama, E.; Nagane, S.; et al. Longitudinal mode control in long cavity VCSELs with a curved mirror. *Appl. Phys. Express* **2022**, *15*, 072009. [CrossRef]
43. Leonard, J.T.; Cohen, D.A.; Yonkee, B.P.; Farrell, R.M.; DenBaars, S.P.; Speck, J.S.; Nakamura, S. Smooth e-beam-deposited tin-doped indium oxide for III-nitride vertical-cavity surface-emitting laser intracavity contacts. *J. Appl. Phys.* **2015**, *118*, 145304. [CrossRef]
44. Lee, S.-G. Demonstration of GaN-based vertical-cavity surface-emitting lasers with buried tunnel junction contacts. *Opt. Express* **2019**, *27*, 31621. [CrossRef] [PubMed]
45. Kiyohara, K.; Odawara, M.; Takeuchi, T.; Kamiyama, S.; Iwaya, M.; Akasaki, I.; Saito, T. Room-temperature continuous-wave operations of GaN-based vertical-cavity surface-emitting lasers with buried GaInN tunnel junctions. *Appl. Phys. Express* **2020**, *13*, 111003. [CrossRef]
46. Shen, C.-C.; Lu, Y.-T.; Yeh, Y.-W.; Chen, C.-Y.; Chen, Y.-T.; Sher, C.-W.; Lee, P.-T.; Shih, Y.-H.; Lu, T.-C.; Wu, T.; et al. Design and fabrication of the reliable GaN based vertical-cavity surface-emitting laser via tunnel junction. *Crystals* **2019**, *9*, 187. [CrossRef]
47. Hamaguchi, T. Highly-efficient operation and mode control in GaN-based VCSELs with a curved mirror. In *Gallium Nitride Materials and Devices XVIII, 124210H*; SPIE: San Francisco, CA, USA, 2023; Volume 12421.
48. Funato, M.; Kaneta, A.; Kawakami, Y.; Enya, Y.; Nishizuka, K.; Ueno, M.; Nakamura, T. Weak Carrier/Exciton Localization in InGaN Quantum Wells for Green Laser Diodes Fabricated on Semi-Polar {2021} GaN Substrates. *Appl. Phys. Express* **2010**, *3*, 021002. [CrossRef]
49. Mei, Y.; Weng, G.E.; Zhang, B.P.; Liu, J.P.; Hofmann, W.; Ying, L.Y.; Zhang, J.Y.; Li, Z.C.; Yang, H.; Kuo, H. Quantum dot vertical-cavity surface-emitting lasers covering the 'green gap'. *Light Sci. Appl.* **2017**, *6*, 16199. [CrossRef]
50. Iida, D.; Kirilenko, P.; Velazquez-Rizo, M.; Zhuang, Z.; Najmi, M.; Ohkawa, K. Demonstration of 621-nm-wavelength InGaN-based single-quantum-well LEDs with an external quantum efficiency of 4.3% at 10.1 A/cm^2. *AIP Adv.* **2022**, *12*, 065125. [CrossRef]
51. Yanagihara, A.; Kishino, K. monolithically integrated green-to-orange color InGaN-based nanocolumn photonic crystal LEDs with directional radiation beam profiles. *Appl. Phys. Express* **2022**, *15*, 022013. [CrossRef]
52. Takeo, A.; Ichikawa, S.; Maeda, S.; Timmerman, D.; Tatebayashi, J.; Fujiwara, Y. Droop-free amplified red emission from Eu ions in GaN. *Jpn. J. Appl. Phys.* **2021**, *60*, 120905. [CrossRef]
53. Michalzik, R. *VCSLEs: Fundamentals, Technology and Applications of Vertical-Cavity Surface-Emitting Lasers*; Springer: New York, NY, USA, 2013; p. 386.
54. Sandanayaka, A.S.; Matsushima, T.; Bencheikh, F.; Terakawa, S.; Potscavage, W.J.; Qin, C.; Fujihara, T.; Goushi, K.; Ribierre, J.C.; Adachi, C. Indication of current-injection lasing from an organic semiconductor. *Appl. Phys. Express* **2019**, *12*, 061010. [CrossRef]